INAF TECHNICAL REPORT

Compatibility studies between Radio Astronomy and three upcoming telecommunication technologies

---

Fabio Giovanardi (INAF-OAA)
Vincenza Tornatore (Polimi)
Benjamin Winkel (MPIfR)
Pietro Bolli (INAF-OAA)

Contact:
fabio.giovanardi@inaf.it

Abstract
In recent years, the increased use of high-frequency technology in the millimetre and microwave range, including mobile phones, automobiles, and industrial equipment, has further reduced and threatened the spectrum assigned to the radio astronomy service (RAS). As a scientific and passive service, RAS requires protection from commercial services to observe the extremely faint celestial signals. As spectrum use for land, air and space communications grows, protecting RAS operations from radio frequency interference is becoming more challenging. This report examines the impact of advanced technologies on radio astronomy, specifically car radar at 77 GHz, 5G and Wi-Fi device deployments at 6.6 GHz. These technologies are evaluated for their potential impact on Italian radio telescopes: the Radio Observatories of Medicina and Noto and the Sardinia Radio Telescope (SRT). Of particular concern is the potential threat posed by car radars to future high-density prospects, as well as the historical importance of the 6.6 GHz frequency for radio astronomical observation of methanol emissions from stars.

1 Introduction

Nowadays, radio astronomy is increasingly requiring protection of the radio spectrum due to the emergence of new telecommunication applications.
While the International Telecommunication Union (ITU) has designated some bands of frequencies exclusively allocated for radio astronomy, it is possible for radio astronomy service to share frequency bands with other services. For that reason, electromagnetic compatibility studies are conducted in order to ensure the feasibility of band sharing. Such studies are also relevant in case of use of adjacent frequency bands between radio astronomy and active services to avoid that out-of-band emissions can compromise the scientific observations.
Radio astronomy is a passive service (it does not emit signals) aimed at receiving very weak signals from the cosmos, and as such it is more susceptible to interference than other services. Furthermore, the spectral emission of the elements is fixed by their nature, reducing the flexibility in setting the parameters to observe the sky. Because of this, it is essential to study the electromagnetic compatibility of different services and take the necessary measures to ensure that services can coexist without interference.
In recent years, three topics have emerged as particularly relevant for the protection of RAS: car radar (also known as automotive radar), the proposed assignment of frequency bands between IMT (i.e., 5G devices) and RLAN (including Wi-Fi) in the upper band of 6.6 GHz. As technology continues to advance, these topics are becoming increasingly important for ensuring effective protection of RAS.
This report aims to provide a comprehensive overview of the compatibility studies conducted at INAF to safeguard national radio astronomy sites. It highlights the impact of upcoming services and the corresponding measures taken to address them. All the studies included in this report have utilized the pycraf [1], a freely available Python package. The findings emphasize the significance of effective frequency management and the proactive response required by INAF to protect radio astronomy sites from potential harm caused by emerging services.
The primary objective of this report is to present a summary of recent compatibility studies examining the coexistence of radio astronomy and upcoming technological applications. European radio astronomers collaborate to conduct these studies. They are subsequently submitted to the European Conference of Postal and Telecommunications Administrations (CEPT) and the Electronic Communications Committee (ECC). These organizations regulate the use of the radio spectrum across Europe. The studies presented herein assess the impact of automotive radar, IMT (5G), and

Table 1: List of the Italian radio telescopes (RT) investigated in this report

Observatory Name	Longitude (E), Latitude (N)	Elevation (m AMSL)	Antenna height from the terrain (m)	Geographical characteristics
Sardinia (SRT)	09°14'42" 39°29'34"	600	32	Partially shielded by surrounding mountains
Medicina	11°38'49" 44°31'15"	28	16	Flat plain near Bologna
Noto	14°59'21" 36°52'34"	90	16	Partially shielded by surrounding mountains

RLAN (Wi-Fi) on radio astronomy observations and ensure the preservation of their integrity.
The studies presented in this report are based on regular work carried out by the Committee on Radio Astronomy Frequencies of the European Science Foundation (CRAF) and reflect the extensive efforts of the expert committee to protect radio astronomy at both the European and international levels. The compatibility studies presented in this report have been selected and reorganized from the official documents submitted to CEPT and the International Telecommunication Union (ITU).

1.1 Italian radio telescopes

The three Italian radio telescope sites: Medicina (the single-dish antenna was recently named after Gavril Grueff), SRT and Noto, have been studied in detail. Table 1 shows geographical information of the three sites, and figure 1 shows their location on a geographical map.

1.2 Frequency management

Frequency spectrum is a limited and public resource regulated by the administrations of each country. Regulation of the radio spectrum is a process that can be viewed at different levels: the international level (ITU), the European level (CEPT) and the national level.
The ITU, a specialized agency of the United Nations, is responsible for different matters related to information and communication technology, including the shared global use of the radio spectrum to direct toward international cooperation. ITU also covers various telecommunication applications such as for satellites, broadband internet, wireless technologies, aeronautical and maritime navigation, radio astronomy, satellite meteorology, television broadcasting, radio amateurs and new generation networks.
Since its establishment in 1865, the ITU with headquarters in Geneva, Switzerland has expanded to include 193 countries and approximately 900 private companies. The Radio Regulations (RR) [2] is the binding international treaty that governs how the radio frequency spectrum is shared between different services, including space and military functions.
The World Radio Conference (WRC) is a significant event held every three to four years, where essential modifications to the Radio Regulations (RR) are discussed on the agenda. Several working groups assist in preparing for the WRC, with the Conference Preparatory Meeting (CPM) playing a crucial role in drafting the comprehensive CPM Report.

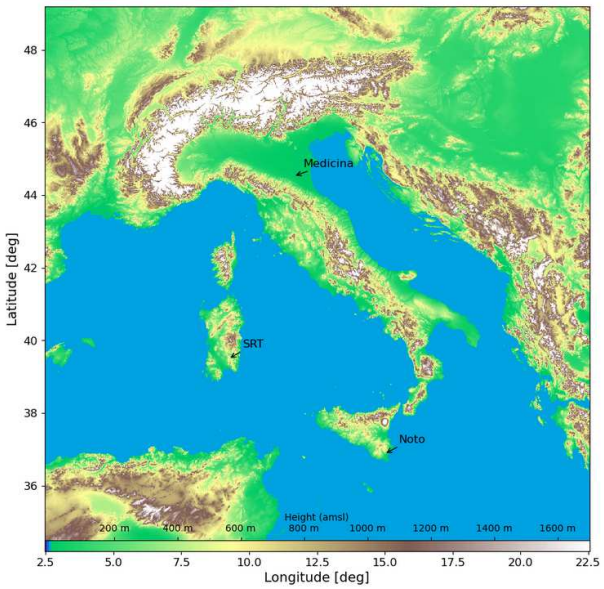

Figure 1: Map of Italian radio telescopes investigated in this report

Within the ITU, three sectors deal with practical and technical issues: radio frequency allocation, satellite orbit management and access technologies (ITU-R); technical standard's development for telecommunications (ITU-T); facilitating and improving global access to information and communication technology, i.e. Development Sector (ITU-D). For radio astronomy, ITU-R is the most significant group, as it is responsible to allocate spectrum to each service. ITU-R consists of six study groups (SGs) that cover a wide range of radio communication topics:

- SG 1: Spectrum management
- SG 3: Radiowave propagation
- SG 4: Satellite services
- SG 5: Terrestrial services
- SG 6: Broadcasting service
- SG 7: Science services

In SG 7, responsible for science services, there are four working groups: WP 7A focuses on terrestrial and satellite systems for disseminating time and frequency signals, WP 7B deals with space radiocommunications applications for telecommand, tracking, and telemetry data, WP 7C covers remote sensing systems for Earth exploration and space research, and finally WP 7D is responsible for the protection of radio astronomy, radar astronomy sensors both on Earth and in space including space very long baseline interferometry (VLBI).
At European level, CEPT, established in 1959 and composed by 48 countries, harmonizes telecommunications, spectrum use and postal issues while improving their effectiveness and coordination in the interest of European consumers. CEPT is organized into three main components:

1. ECC oversees radiocommunications and telecommunications matters, it was formed with the merger of European Committee for Telecommunications Regulatory Affairs (ECTRA) and European Radiocommunications Committee (ERC). The ECC's permanent secretariat is the European Communications Office (ECO).
2. CERP (European Committee for Postal Regulation) is responsible for postal regulation.
3. CEPT coordination is the responsibility of the committee for ITU Policy (Com-ITU) during the preparation and performance of the ITU activities council meetings, plenipotentiary conferences, World Telecommunication Development Conferences and World Telecommunication Standardization Assemblies.

Internally, ECC is composed of several groups:

- WG Frequency Management (WG FM)
- WG Spectrum Engineering (WG SE)
- Conference Preparatory Group (CPG)
- ECC PT1 "IMT matters"
- TG 5 "ECC Structure"

WG FM is responsible for formulating strategies, plans, and recommendations regarding the management of the radio spectrum. On the other hand, WG SE focuses on developing technical guidelines and compatibility arrangements for the use of the radio spectrum by various radio communications services.
Finally, at national level, the Ministry of Enterprises and Made in Italy (MIMIT, ex MISE. is the main body responsible for managing Italy's radio spectrum. Its main activities include the drafting and updating of the National Plan of Frequency Allocation (PNAF), the promotion of the efficient use of the spectrum, the management of interferences, the representation of Italy in international offices for the planning and management of frequencies and the signing of frequency coordination agreements. It also ensures that all services use spectrum harmoniously, promotes access to spectrum for new users and encourages technological innovation.
The Committee on Radio Astronomy Frequencies (CRAF) is a European association of radio astronomers and observers, it was originally established in 1988 to protect the RAS in Europe. This committee has two primary missions: to keep RAS frequency bands free from interference and to ensure that the radio spectrum is available for scientific purposes. RAS is a passive service that doesn't interfere with other radio spectrum users and contributes to our understanding of the universe. However, the increasing use of the spectrum for land, air and space communications poses challenges to radio astronomy operations protection from interference. CRAF serves as an observer at CEPT and as a sector member at the ITU. Its goal is to protect radio frequency bands.
In the field of telecommunications, radio astronomy is recognized as a service, but it is passive in nature, involving no active signal transmissions. Within the spectrum, specific frequency bands are allocated to radio astronomy, each with varying priority levels, either primary or secondary. It is essential to note, however, that radio astronomy is provided with special protections under the Radio Regulation. Some examples are bands that require protections as important observations are made (defined in 5.149) and the passive bands where all emission from any service is prohibited(outlined in 5.340).

1.3 Compatibility studies

The purpose of compatibility studies in radio astronomy is to evaluate and mitigate potential interference resulting from a variety of sources, such as wireless communication systems and satellite networks. These studies are typically classified into two categories: single interference and aggregated interference assessments. Single interference studies focus on scrutinizing the impact of specific sources or services on radio astronomy observations, often assuming a worst-case scenario where the transmitting devices are pointed directly at the radio telescope. In contrast, aggregated interference studies adopt a more comprehensive approach, examining the cumulative effects of numerous sources and services operating within the same frequency bands. These studies are considerably more complex, often requiring in-depth knowledge of transmitter deployments, which can be either statistically determined or precisely known.
These studies contribute to the integrity of radio astronomy observations, to the harmonious coexistence of diverse technologies, and to the preservation of high-quality standards in scientific research in this area.
The studies presented in this report are conducted using the open-source Python package pycraf [1], which was developed by CRAF for the studies of electromagnetic compatibility, especially for radio astronomy studies.
It provides a comprehensive suite of tools and features that allow researchers and engineers to model and analyse the propagation of electromagnetic waves in various scenarios. Among the key features of pycraf there is the implementation of the ITU's official path propagation model. This model allows users to simulate the propagation of electromagnetic waves in different environments, including free space propagation, diffraction, earth curvature and atmospheric absorption. Pycraf also allows a complete integration with terrain datasets, which can be used to model the impact of terrain on signal propagation and interference. Furthermore, pycraf is particularly useful for conducting complex analyses, such as full Monte Carlo simulations for aggregation scenarios with thousands of transmitters emitting power. This makes possible to evaluate the performance of communication systems in realistic and challenging scenarios, where multiple transmitters are operating simultaneously and interference can be a significant issue. The tools included in pycraf can calculate link budgets, estimating interference levels. Pycraf also includes a variety of visualization tools enabling users to visualize the propagation of electromagnetic waves in different scenario. Moving forward, CRAF plans to continue expanding and enhancing pycraf, making it an even more valuable tool for radio astronomy data analysis and processing.

2 General considerations about compatibility studies

Propagation models are essential for estimating the attenuation of a signal along its path at a given frequency. The path loss in free space can be considered as a first approximation, and this depends on the distance between the transmitter and receiver and the frequency. To improve accuracy, obstacles, and therefore signal diffraction, can be introduced in the propagation model. ITU recommends a complete propagation model, Rec. ITU-R P.452-16 [3] which considers the earth curvature and physical phenomena such as tropospheric scattering and surface ducting. Signals can travel through the atmosphere, overcoming terrain loss and covering long distances via elevated layer reflection and refraction, which can be significant over quite long distances (up to 250-300 km).
Furthermore, atmospheric attenuation defined by ITU-R 676 [4] also contributes to signal weakening. This method employs frequency, atmospheric characteristics, and path geometry to predict attenuation levels. Oxygen and water are the two primary components that cause attenuation. Oxygen produces the non-resonant Debye spectrum below 10 GHz, while nitrogen causes continuous

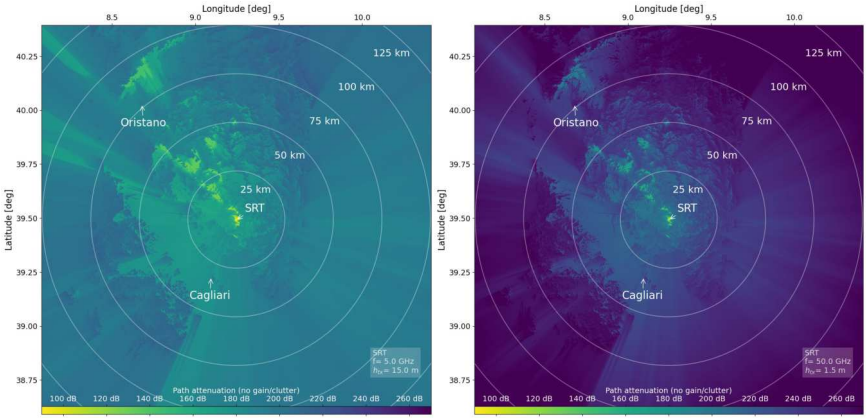

Figure 2: Comparison of attenuation maps in the area around the SRT observatory at different frequencies and 5GHz (left) and 50GHz (right)

attenuation above 100 GHz.
To determine atmospheric attenuation, raytracing models the atmosphere into several hundred layers. The incoming signal is attenuated in each layer, resulting in an outgoing signal weaker than the incoming one. Additionally, each layer emits radio waves with distinct spectral characteristics. To compute the specific attenuation for each layer, unique physical properties such as temperature, pressure, water content and refractive index must be considered. For ITU-R studies, average physical properties over a year are typically used. ITU-R P.835 [5] provides a "standard profile" and five specialized profiles based on geographical latitude and season, including "high-latitude summer/winter", "mid-latitude summer/winter" and "low-latitude".
As an example, Figure 2 shows a comparison of attenuation maps around the SRT site by varying the frequency of the transmitter.

As well as propagation path and atmospheric attenuation, also obstacles such as buildings and vegetation can affect signal attenuation. The amount of attenuation due to these obstacles is called clutter loss. To properly estimate clutter loss, Corine Land Cover (CLC) data [6] is used in pycraf to determine the clutter zone types for each position along the radio path.
CLC is a European project that focuses on the detection and monitoring of land cover and land use characteristics. The database classifies the map into up to 44 categories, with each category corresponding to a specific level of attenuation. For aggregated simulations, where the contribution of individual transmitters depends strongly on their position on the map, this database is suitable. However, since CLC defines clutter "classes" with a finer granularity than model P.452, a conversion has to be made. Using the model in Rec. ITU-R P.452, the clutter loss for each simulation device can be calculated. The accuracy of maps is crucial for compatibility studies because the height of the transmitter can have a significant impact. Additionally, the ITU-R P.452 clutter classes "Sparse", "Deciduous Trees" and "Coniferous Trees" are assigned to Rural zones, the "Suburban" and "Industrial Zone" clutter classes are assigned to Suburban zones, and the "Urban" clutter class is assigned to Urban zones. It is important to note that this model is not purely derived from physics but is instead based largely on empirical modelling. This approach is the result of analysing data from numerous measurement campaigns to obtain the most accurate results. The

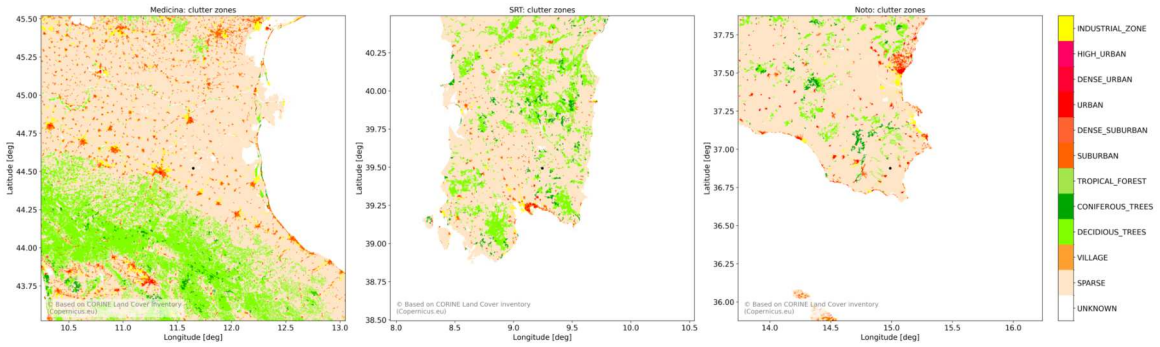

Figure 3: Clutter zones of Italian RTs according to classification of CORINE dataset

clutter zones around Italian radio telescopes are illustrated in Figure 3. The urban environment is represented by red, while the natural environment is represented by green, and the rural environment by light pink. Aside Rec. ITU-R P.452, ITU-R P.2108 provides a statistical distribution of clutter loss for urban and suburban environments.
This method should not be used if the propagation model incorporates clutter losses. According to ITU-R P.2108 the clutter loss depends only on frequency, distance, and a quantity called location percentage, p_L, which is the percentage of emitters with the lowest clutter loss. However, distance dependence is only relevant for small values (below 2 km).
Another factor that can contribute to signal attenuation is building entry loss. This type of loss occurs when a signal passes through walls, floors, or ceilings of a building. To estimate building entry loss, the ITU-R P.2109 recommendation provides a method that is commonly used for indoor applications. It helps to quantify the amount of signal attenuation that occurs as a signal penetrates through building materials.

2.1 Terrain dataset

To apply the path propagation model described in ITU-R P.452-16, information about terrain profile is required. This information can be obtained from a geographic database (GIS), which provides an elevation grid on a map with a specific resolution. Lidar data is preferred for obtaining high-resolution terrain height maps for RAS stations in Europe [7, 8], but SRTM data with lower resolution is often used in other regions [9]. For lack of free data, the SRTM data was used only for Medicina [10]. An example of this is shown in Figure 4, which displays the terrain height map for the SRT observatory and a height profile between the site and a generic point. The simulated area in this case is 2 degrees, which equates to approximately 200 km by 200 km.

2.2 Protection criteria

ITU-R has published a recommendation, ITU-R RA.769 [11], which provides guidelines for determining harmful interference levels. In particular, it provides values of power flux density and spectral power flux density limits for representative radio astronomy bands across the spectrum, both for continuum and spectral line observations. Observations measuring the power received from a single antenna are subject to these values. To provide an understanding of the maximum power levels a station can receive without interference, they range from -155 dBm to -177 dBm.

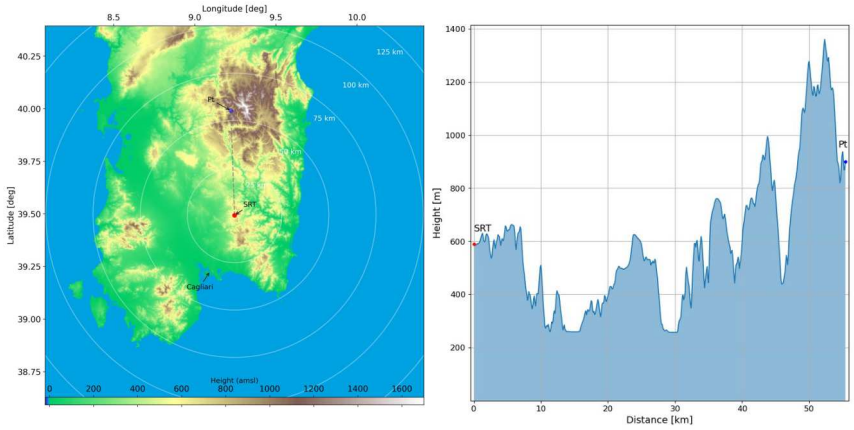

Figure 4: Terrain map of around SRT site. Left, Digital Terrain Model (DTM) with LiDAR dataset [8]. Right height profile between SRT station and a generic point in the map (lat.= 39.990901°, long.= 9.222604°

Despite being in place since 1979, the values have not changed due to the need to protect radio astronomy. Coordination zones are typically used to ensure compatibility between active services and observatories. Another recommendation relevant to radio astronomy protection is ITU-R RA.1513 [12], which specifies that interference caused by other radio frequency services should not result in more than 2% data loss. This is calculated as the percentage of time observed data is unusable due to interference. When evaluating the size of coordination zones, it is critical to note that the distributions of received power levels from all simulations should not be reduced by another 2%. Instead, the mean or median value should be used. Another approach would be to vary the percentage of time value for each device involved in the simulations and apply the 2% limit to the aggregated results. However, this approach is unrealistic, as the relative strengths of radio wave propagation effects should not vary widely over the time span of a typical radioastronomy observation. Typically, scientists who are granted observation time are assigned a fixed time slot, and if radio propagation conditions are particularly favourable during that slot, the entire observation may be lost. Scientists are rarely compensated for this loss.
To properly compute the zone, typically is necessary to compute the minimum coupling loss (MCL) defined as the minimum level of signal attenuation required to ensure compatibility between the two services. In other words, MCL is defined as the difference (in dB scale) between the EIRP of the transmitter and the threshold limitation given by Rec. ITU-R RA.769 for RAS.
The difference between the MCL and the predicted path propagation loss is known as the margin. Positive margins indicate that the received signal strength is less than the RAS threshold from Rec. ITU-R RA.769 and thus both applications are able to coexist. Negative margins indicate a violation of the threshold levels. Therefore, the zero-margin contour indicates the potential size of coordination zones, which are calculated by an algorithm that considers hypothetical transmitters pointing towards the radio telescope for each pixel of the area around the astronomical site. While this algorithm assumes that a transmitter emits from every location with the maximum antenna gain, it still provides a valuable initial assessment. Additionally, ITU-R RA.769 is recommended to assume zero dB antenna gain from side lobes and an integration time of 2000 s. In Table 2, threshold levels are presented for each application investigated in this report. Note that the frequency 6.6 GHz is not in the ITU-R RA.769, but is protected by the note No 5.149 in the ITU Radio Regulations. The

Table 2: Threshold interference levels for application studies in this report

		Threshold interference level (according to ITU-R RA.769)		
frequency	**Application under test**	**Observation type**	**Input Power (dBm) according to the bandwidth specified**	**Spectral Power Density (dBm/MHz)**
6.6 GHz	IMT, RLAN	spectral-line (50kHz)	-188	-175
77 GHz	Car radar	continuum	-159	-198

RAS bands in are 76-81 GHz, while the note No 5.149 protect the band 6650-6675.2 MHz.

3 Compatibility Study between Car Radar and RAS

Car radar is a crucial technology for autonomous driving systems, providing accurate environmental perception for real-time decision-making. Equipped with sensors inside and outside the vehicle, car radars enhance safety by enabling actions such as braking or deceleration to avoid collisions without the need for driver input. As car technology advances, electric cars with autonomous driving assistance have become increasingly popular, requiring the installation of numerous sensors, including radars and cameras, to enable this feature. After a temporary allocation in the 24 GHz band, the car radar allocation is now moved to the 77 GHz band (see ECC Decision (04)10 for details [13]) with improved performance (mainly on resolution and speed). In this report, a compatibility study is carried out with respect to RAS and car radar in the 77 GHz band. In particular, the car radars are now sharing the same band allocated to radioastronomy: 77 – 81 GHz, with primary and secondary status. A lot of work has been done in the last year on compatibility between car radar and other services as RAS, as reported in ITU-R M.2322-0 [14] and ITU-R RA.2457-0 [15]. With respect to previous studies, the study presented in this report provides an exhaustive analysis of car radar compatibility with RAS, incorporating both single and aggregated data. The latter considers hundreds of cars in a specific area around the radio telescope, providing a rather realistic scenario. This study has also been presented at the CEPT SE24 and incorporated into the ECC 350 Report [16].

3.1 Scientific interests and regulatory status of the 77 GHz band

The Radio Astronomy Service is designated as the primary service in the 76 GHz – 77.5 GHz and 79 to 81 GHz frequency bands, with 77.5-79 GHz allocated as a secondary service. The full frequency range (76-81 GHz) is of great scientific interest and is addressed in the footnote RR No. 5.149 which encourages administrations to take all possible steps to protect the service from harmful interference. Leading radio telescopes such as the 30-m radio telescope (IRAM Pico Veleta, Spain), the NOEMA interferometer (IRAM Plateau de Bure, France), the Onsala 20-m radio telescope (OSO, Sweden), and the 40-m radio telescope (IGN-Yebes Observatory, Spain) have been utilized to detect interstellar molecules such as CH3OH, CH3C5N, HC3N, HC9N, C3N, and C5H, among others. The N2D+ J=1-0 line at 77.1 GHz is especially significant since it traces pre-stellar condensations, particularly during the star formation phase when the interstellar gas is still cold. The frequency range of 76-81 GHz is also used for studying the emission of galaxies through highly redshifted CO lines, which is necessary to comprehend star formation inside galaxies.

3.2 Compatibility study

In the near future, cars are expected to be equipped with multiple radars to serve various purposes. The radar configuration will include one type A (or B) radar positioned in the front direction and four type B (or C) radars placed in the corner directions. As for other radar types with shorter ranges, their contribution to the results is considered here negligible.
This study analyses three types of car radar configurations: front radars, corner radars, and a combination of both. The mean Effective Isotropic Radiated Power (EIRP) limit determines the maximum power output of the transmitter. The model implemented in this study considers the pointing direction of the radar transmitting antenna with respect to the position of the radio telescope. In simple terms, radar technology works by sending out short bursts of radio pulses that bounce off objects and return as echoes. For simplicity, this study only considers transmitter power,

Table 3: Car radar classification

Sensor Range	Main Applications (depending on manufacturer)	Radar Type	Modulation Bandwidth	Mean EIRP limit (D= 100%)	Mean EIRP limit (D= 30%)
Long Range (150 – 200 m)	AAC, Collision Warning, AEB	A	Up to 1 GHz	40 dBm	34.8 dBm
Mid-Range (30 – 70 m)	BSD, LCA, RTCA	B	Up to 2 GHz	37 dBm	31.8 dBm
Short Range (< 30 m)	Parking Assistance, Pedestrian Detection	C, D, E*	Up to 4 GHz	30 dBm	24.8 dBm

Note: AAC: Adaptive Cruise Control; AEB: Automatic Emergency Braking; BSD: Blind Spot Detection; LCA: Lane Change Assist; RTCA: Rear Cross-Traffic Alert

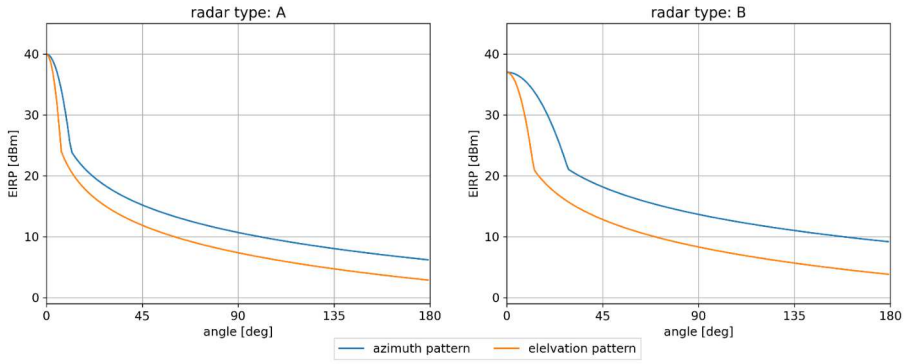

Figure 5: Antenna patterns of type A and B considered in the study (D= 100%

ignoring reflection from nearby metallic objects such as cars or obstacles (terrain reflections are already considered in the ITU-R P.452 propagation model). In table 3 are classified power levels into four categories (A to E) according to Rec ITU-R M.2057 [20]. Typically, radar signals are modulated, and the duty cycle is below 50% (with a 30% assumption in this study). Figure 5 illustrates the antenna patterns of both radar type A and B in both the azimuth and elevation axes.
The compatibility study was done considering two scenarios: single and aggregation interfere scenario. In the first case, the transmitter pointing to the radiotelescope (victim) would be positioned everywhere. In the second case, the analysis performed is more realistic and accurate because the cars are displaced in the actual roads around the radio telescope. The position, clutter losses, and the antenna pattern of each radar are considered in this case.

3.2.1 Single case scenario

In the single case scenario, a single transmitter is used to emit signals towards the RAS station. For this scenario, only type A radars are considered as the transmitter and a duty cycle of 30% is assumed. According to ITU-R RA.769 the RAS threshold is equal to –189 dBW. By doing calculation, the MCL is given to 194 dB.
In Figure 6, the solid line identifies the minimum separation distance for the specific site, based

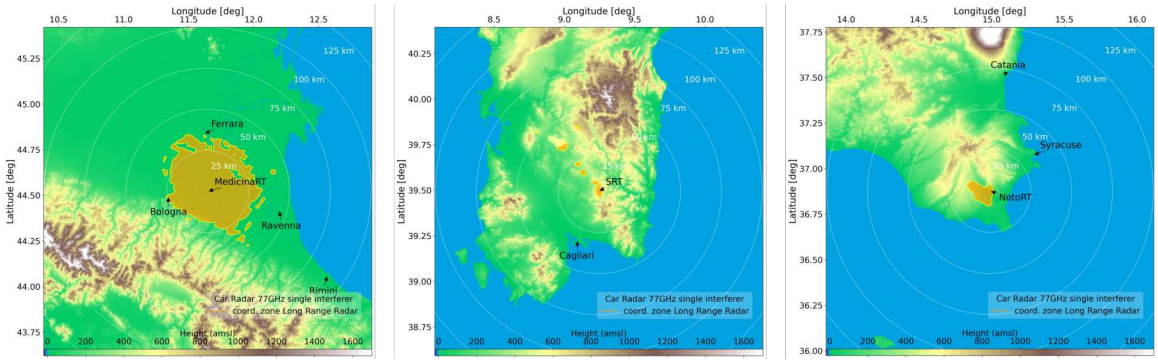

Figure 6: Car Radar exclusion zone for Italian radiotelescope considering a single interference case

Table 4: Vehicle densities (mean and standard deviation) used for the simulation for each road types. Data provided by ECC report 327.

Road type	**Vehicle density (number of vehicles per kilometre, 1/km)**
Primary	3.6 ± 0.9
Secondary	0.6 ± 0.15
Tertiary	0.2 ± 0.05
Residential	0.1 ± 0.025
Other	0.1 ± 0.025

on terrain profile. The white circles show distances from the RAS stations in steps of 25 km. As explained above, the single case scenario is a worst-case study where no clutter attenuation is considered. Given the flat terrain around it, the Medicina site is the most problematic with a coordination zone of over 25 km in each direction assuming only one transmitting device. For SRT site, excluding the north-west direction, the estimated coordination zone is about 8 km. Coordination zones at the Noto site limited to about ten kilometres around the site, demonstrating effective protection against interference.

3.2.2 Aggregated scenario

For the aggregation case, a more realistic scenario is assumed; several vehicles are randomly located on the different roads around the radio telescopes following a statistical distribution (see Table 5). To simulate a realistic distribution of vehicles, road map data from OpenStreetMap [17] (OSM) is utilized as an API, which is available under the Open Database Licence [18]. For each scenario, road map data within an area of 200×200 km are queried. OSM differentiates between various road types, classified as “primary”, “secondary”, “tertiary” and “residential” according to the estimated density. Other roads are included in the “other” category. Table 4 shows the vehicle density at a given road type.

However, a report [19] indicates that the car density in Europe is higher than what was assumed in this report, which therefore presents an optimistic scenario. When interpreting the numbers, one should consider that different types of roads would have very different traffic statistics. The

Table 5: Total Road length per road type in a square area of 200×200 km, centred on the RAS stations.© OpenStreetMap's contributors.

Road Type	Total length of roads (per type) (km)		
	SRT	Medicina	Noto
Primary	3,981	11,804	2,976
Secondary	4,130	15,793	5,419
Tertiary	4,858	22,464	9,674
Residential	9,052	41,604	15,839
Other	10,389	59,909	13,752
All	32,410	151,573	47,661

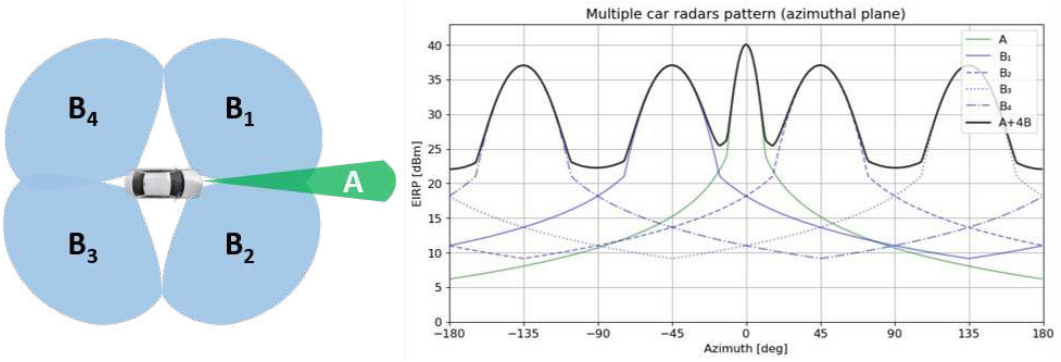

Figure 7: Antenna pattern of multiple radars (duty cycle = 100%), type A in the front direction and 4 type B in the corner directions at 0° elevation plane. Left: top view of the radar distribution.

Medicina station, for example, has over 11,000 km of primary road network in the area analysed, thus involving numerous vehicles examined.

For an aggregation study, one can create samples of vehicles that follow the road distribution and account for the different types of roads. To acknowledge the fact that traffic can be different during the day (and night) and from day to day, the overall number of vehicles in such a sample is varied. In Table 5 the deployment parameters are summarized. In total, the simulation was repeated 100 times to have a fair number of realizations for statistical analyses, e.g., to estimate uncertainties. In each simulation, vehicles were randomly placed on the roads according to the desired density distributions. The antenna pattern provided by ITU-R M.2057 [20] is applied to determine the effective gain of the transmitter in the direction of the RAS station. The EIRP patterns are shown in Figure 7. The resultant antenna pattern for the mix A+4B scenario is illustrated in Figure 8.
Figure 9 provides a visual representation of the simulated car distribution for each station. The average car density per square kilometre is 6.7, 2.0, and 1.9 for Medicina, SRT, and Noto stations, respectively. Transparent lines indicate the road, while filled dots show the positions of vehicles (note that due to the high density of cars on primary roads, red dots may be difficult to distinguish). RAS stations are marked with black squares, and grey circles at 25 km intervals denote distances from the stations.
Based on the location of vehicles, one determines the propagation loss individually. Furthermore, the Corine Land Cover (CLC) is queried to obtain the clutter type zones for each position. Based

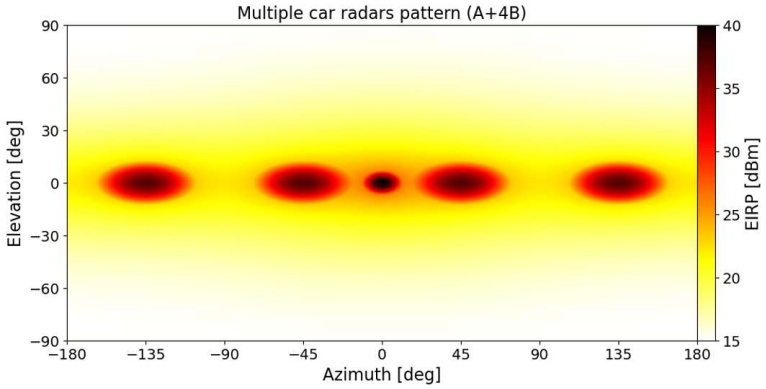

Figure 8: Antenna pattern of multiple radars (duty cycle = 100%), type A in the front direction and 4 type B in the corner directions, displayed for both azimuthal and elevation planes.

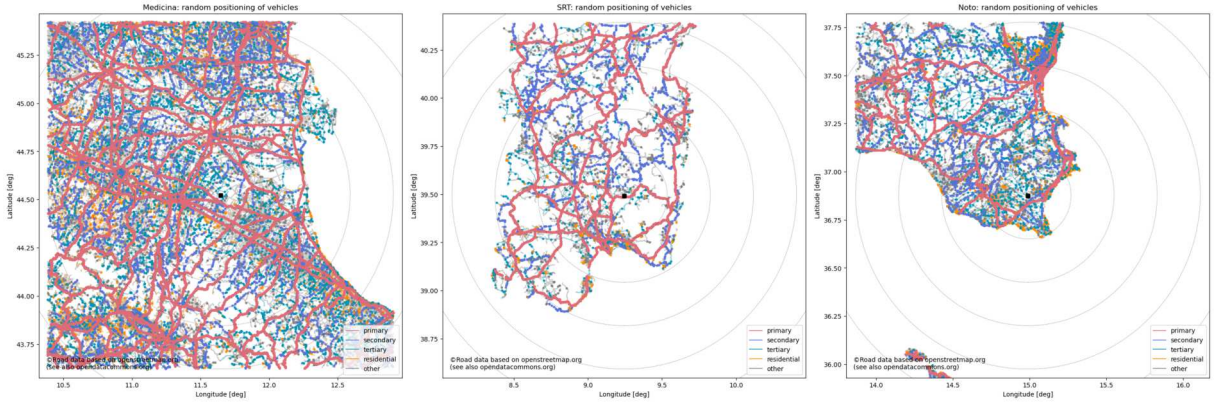

Figure 9: Random vehicle positions from the simulations around Italian RAS stations

on the clutter type, the clutter loss model in Recommendation ITU-R P.452 [3], and a TX height of 0.7 m, the clutter loss could be determined to show the inferred clutter types around each station.
The aggregate simulation using Monte Carlo method involves running multiple iterations, each with different configurations of car distribution in the designated area, to emulate high or low traffic scenarios. The emitted power levels of each car are summed up to calculate the received power level at the RAS station, accounting for antenna gains and propagation losses.
To determine the minimum separation distance between the RAS and wireless devices, the received power is evaluated for different separation distances (coordination radius) Ri. The total contribution of devices located inside a circular area of radius Ri is subtracted from the power calculated using the full map, generating curves of received power versus separation distance. The median of the distribution is obtained by analysing the 50th percentiles, and the minimum separation distances are identified by the intersection of the median curves with the threshold power level for harmful interference recommended by ITU-R RA.769.
The results are depicted in Figure 10, which show the received power for the various coordination zones for each iteration and the median for single radar (type A) and multiple radars (A+4B).
The results show a range of necessary coordination zone sizes, depending on the radar config-

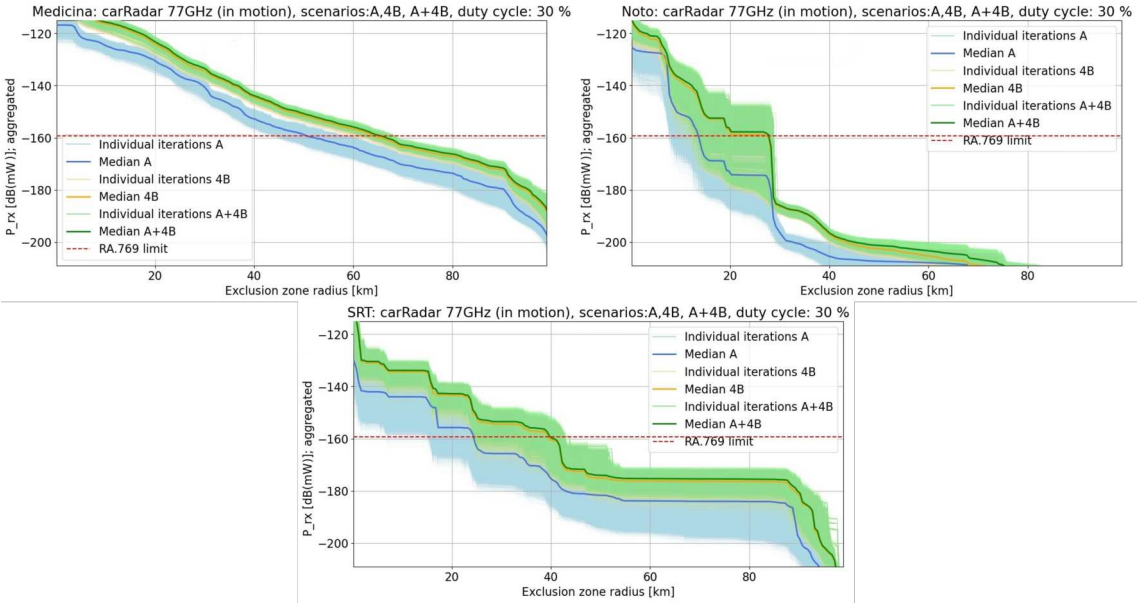

Figure 10: Results of the aggregation calculation of Automotive Radar with duty cycle= 30%

uration and environment of a site. The spread of curves is due to the high number of possible configurations considered. As a result, the front radar scenario is compatible with RAS with a coordination zone size of about 50 km for the Medicina station, 24 km for the Sardinia station, and 13 km for the Noto station, respectively. However, when multiple radars (front and corner) are considered, the coordination zone size increases to 65 km (Medicina), 40 km (SRT), and 27 km (Noto). Additionally, corner radars alone provide a larger coordination zone than front radars despite having a lower peak power because they cover a wider area. Table 6 shows a summary of the necessary coordination zone sizes for the different radar configurations, with a comparison between single case scenarios for front radar.

Table 6: Summary of the coordination zone radius for the Italian RT with D= 30%

	Coordination zone (km)			
Observatory Name	**Single case scenario**	**Aggregated case scenario**		
	Front radar	**Front radar**	**Corner radars**	**Front + corner radars**
Medicina RT	30	50	64	65
SRT	8 (up to 50 km in one direction)	24	39	40
Noto RT	15	13	20	27

4 Compatibility Study between IMT and RAS

The upcoming WRC in Dubai at the end of 2023 will address new requests for radio spectrum from mobile operators, also known as International Mobile Telecommunications (IMT). IMT includes not only emerging technologies such as Internet of Things (IoT) and machine to machine communications (M2M), but also commercial wireless technology and service infrastructure that encompasses a broad range of communication options, including 2G, 3G, 4G, and 5G.

4.1 Scientific interests and regulatory status of the 6.6 GHz band

ITU identified a proper agenda item (AI1.2) to the next WRC-23 aiming to assign IMT the use of the high-end 6 GHz band. In particular, under AI1.2 ITU will analyse several frequency regions for possible allocation to IMT: 3300-3400 MHz, 3600-3800 MHz, 6425-7025 MHz, 7025-7125 MHz, and 10.0-10.5 GHz. For RAS, the most problematic band is 6425-7025 MHz. This is because methanol line is emitted at 6668.518 MHz, and measurements of this band play a major role in star formation research. This is the frequency where the study presented in this report is conducted. One of the fundamental building blocks of life, methanol (CH), was the first molecule discovered in the interstellar medium. In star-forming regions such as the Orion Nebula, it is abundant; by observing it, we can learn about circumstellar shells and the dynamics of star-forming regions. The methanol molecule is used to study maser emission in regions that are forming massive stars. In addition to studying the structure of our galaxy, this is accomplished through the study of stars, their evolution, age, and dynamics. In addition, methanol observations have been used to determine the length of the spiral arms of the Milky Way, which was not previously known.
Besides the in-band signals, RA observatories are also susceptible to out-of-band emissions (OOBE) from mobile devices. To assess the impact of IMT on RAS, both OOBE and aggregate emissions from multiple IMT devices must be analysed. The aggregate emissions from multiple IMT devices could result in harmful interference, even though a single emission may not have a noticeable impact on a RAS station. Therefore, evaluating the combined effect of all emissions from numerous IMT devices on RAS, considering their spectral characteristics and the geographical location of both the RAS station and the IMT devices is crucial. However, in this band, atmospheric loss is relatively small, and the majority of attenuation is caused by distance.
The RAS band 6650-6675.2 MHz is already protected by footnote RR No. 5.149, “administrations are urged to take all practical steps to protect radio astronomy services from harmful interference”, meaning that the protection of astronomy is not mandatory and left to the decisions of national authorities. However, a secondary status is assigned to RAS in Italy in this band.

4.2 Compatibility studies

There are many online articles that discuss the various features of 5G technology, but most of them focus solely on telecommunications performance and fail to address compatibility issues. When comparing 5G to its predecessor, 4G (also known as LTE), there are several practical differences worth noting. For example, 5G antennas typically use active antenna arrays (AAS) with fewer elements than the traditional passive antennas used in 4G. This is due to beamforming technology employed by AAS, which enables more focused signal transmission with fewer antenna elements. By combining beamforming and MIMO technologies, a large number of users can be efficiently served, improving spectral efficiency, and increasing signal-to-noise ratios. However, it is important to note that claims that this technology reduces interference by focusing the antenna pattern on the receiver may be oversimplified. Both User Equipment (UE) and Base Station (BS) use MIMO

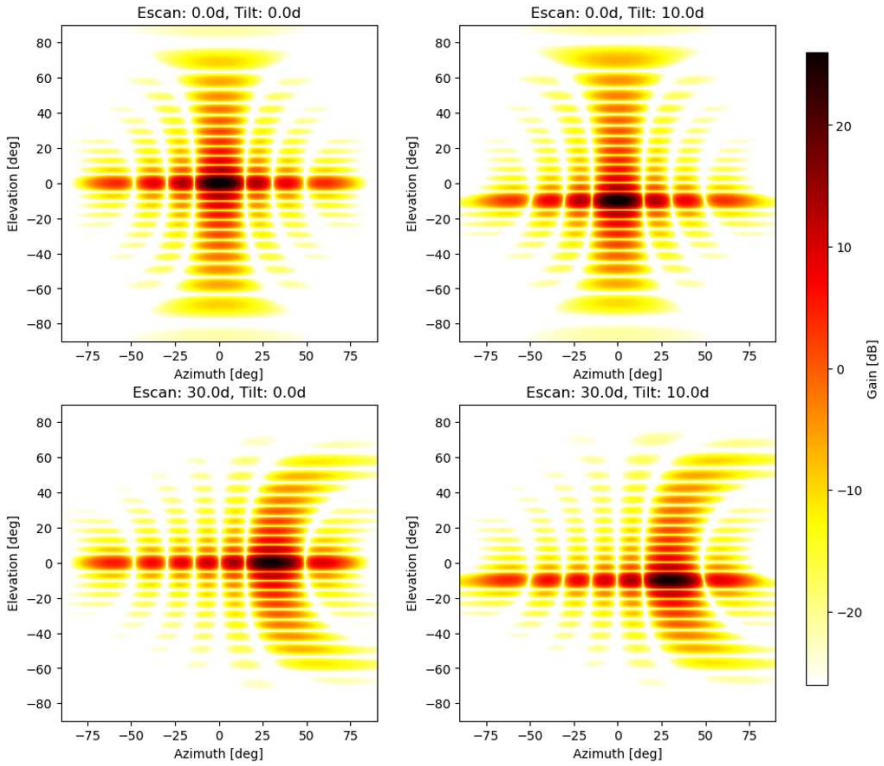

Figure 11: Typical antenna pattern for 5G devices. As an example, four beam steering directions are shown.

and beamforming technologies. A typical 5G antenna for the Base Station (BS) is shown in Figure 11 in four orientation directions.
Moreover, UE employs a power control algorithm to regulate the power transmitted to the BS. This feature, also present in 4G systems, can reduce terminal consumption, and optimize power usage. The power control algorithm adjusts the UE's output power based on factors such as the distance between the UE and the BS and the type of route being used. By increasing or decreasing the output power, the algorithm ensures that the UE uses the minimum amount of power required to maintain a strong connection with the BS. The power control algorithm is modelled in accordance with Rec. ITU-R M.2101, which provides guidelines for designing and implementing IMT systems. Ultimately, this feature helps to optimize power usage and extend UE battery life.
CRAF presented a compatibility study with IMT to the ITU 7D group, but it was not accepted due to the fact that only primary services are permitted to contribute to WRC-23. Even so, the study was submitted to PT1 at CEPT [21]. In this study, both single and aggregate cases are examined. The study resulted in exclusion zone estimation with respect to IMT in which sharing, adjacent band and spurious domain scenarios are investigated. A case of study of site-specific single case of Italian radiotelescopes is shown.
In combination with a propagation model ITU-R P.452-16, ITU-R P.2108 clutter loss (the loss due to vegetation and buildings) is considered. Assuming flat terrain (an equivalent spherical Earth model with zero ground elevation, where the Earth's curvature is considered), the 6.65 GHz path

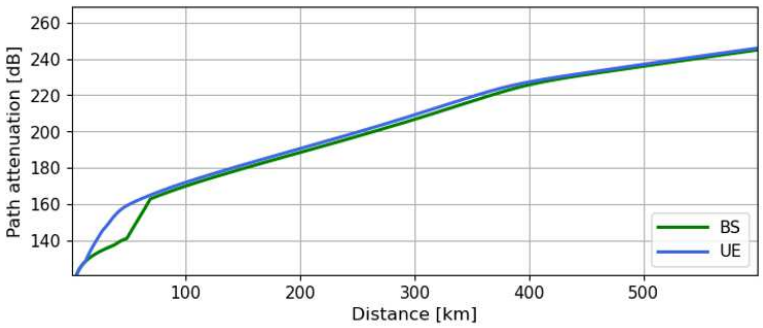

Figure 12: Path attenuation of UE and BS with a flat terrain assumption (flat earth model)

attenuation depends on the associated area (defined as urban, suburban, or rural). Since radiotelescopes are typically located in remote areas, the analysis considers only rural settings for the single case. The resulting path attenuation values for (UE) and (BS) are presented in Figure 12. As expected, the path attenuations exhibit a consistent monotonic trend. Both curves show similar behaviour, but the discrepancy between about 20 and 80 km is due to the large height difference between the base station (25 m) and the user (1.5 m).
The technical parameters of the IMT system used in this study are adopted from the 716th meeting of ITU WP-5D, the group dedicated to IMT systems. The parameters of the antenna and the model of the IMT network are listed in Table 7 in accordance with the recommendation in Rec. ITU-R M.2101-0 which are drawn specifically for the purposes of compatibility studies between IMT and other applications. Moreover, the base stations are usually not operating at 100% of their maximum capacity. In the calculations, a reasonable network-loading factor of 20% is assumed. The time division duplex (TDD) activity factors are 75% for base stations and 25% for user equipment.

4.3 Single case scenario

The generic single-interferer case is the situation of a BS or UE pointing directly at the RAS station, which is the worst-case scenario. Figure 13 shows the exclusion zone of single interference (in-band, adjacent and spurious scenario) for a generic radiotelescope computed without considering any terrain profile. The station's height is assumed to be 32 meters.

The coordination zones obtained range from 65 km and 400 km respectively for UE and BS for the sharing condition to 14 km and 106 km for the spurious scenario (for brevity it is not shown here). In order to estimate the impact that it would have on the Italian radio telescopes, the terrain profile is introduced for each Italian site. Figure 14 illustrates the coordination zone for Italian radiotelescopes based on in-band conditions, considering clutter loss and no clutter loss. As a worst-case scenario analysis, the simulations presented in the single case scenario should not consider clutter loss. This is because BSs are usually installed at high elevations above vegetation and roofs to provide a broad coverage area. However, it is shown as comparison to the impact of clutter loss, which compares the loss with (blue curve) and without clutter (red curve).

Table 7: IMT parameters

Parameters	IMT Base station	IMT User equipment
Band parameters		
Frequency	6.65 GHz	6.65 GHz
Carrier bandwidth	100 MHz	100 MHz
Antenna parameters (Rec. ITU-R M.2101-0)		
Antenna pattern[1]	*Rural* 8 × 16 × 2 array elements (H+V) G_{elem} = 6.4 dBi	-4 dBi (avg. isotropic) Single element
Beamforming efficiency[2]	ρ = 1.00 (in-band) ρ = 0.95 (adjacent) ρ = 0.80 (spurious)	n/a
Antenna down-tilt	6° (Rural)	n/a
Antenna height	25 m (Rural)	1.5 m
Emitted powers		
Ptx (emitted power)[3]	22 dBm per element	23 dBm
EIRP [4]	73.55 dBm (Rural/ Macro Sub-urban)[27]	19 dBm
Conducted spectral power density (Total array, without gain)	26 dBm/MHz (in-band) -4 dBm/MHz (adjacent) -30 dBm/MHz (spurious)[3]	3 dBm/MHz (in-band) -7 dBm/MHz (adjacent) -30 dBm/MHz (spurious)
Power into RAS frequency band (Spectroscopy channel width: 50 kHz)	13 dBm (in-band) -17 dBm (adjacent) -43 dBm (spurious)[3]	-10 dBm (in-band) -20 dBm (adjacent) -43 dBm (spurious)
Network loading factor[5]	20%	n/a
TDD activity factor[5]	75%	25%
Deployment		
Deployment density in hotspot area (number of sectors; 3 sectors per BS position)	0.006 km^{-2} (Rural)	3 UEs per BS sector
Fraction of indoor devices	n/a	50% (Rural)
Distribution of user equipment (relative to base station)		
BS cell radius	0.9 km (Rural)	
Distance distribution	Rayleigh(0, 300) (Rural)	
Angular distribution	Normal(0, 30) (clipped at ±60°)	

[1] Annex 4.4 to Working Party 5D Chairman's Report, [22]. Transmitter and antenna parameters are also explicitly defined within the ETSI document as suburban macro scenario.[27].

[2] Composite antenna pattern (beamforming) efficiency is still significant in adjacent and (near) spurious domain; [24]. However, the values that are used for ρ in this study were not specified in Doc. 5D/716 (Annex 4.4) [22].

[3] Using Category-B limits [22].

[4] EIRP is not taken into account in this study as it is the antenna pattern is even considered for both single and aggregation cases.

[5] Rayleigh's distribution for radial distance (UE-BS) sampling was proposed by Task Group 5/1 Chairman's Report [22] for open-space suburban hot-spots in compatibility studies of WRC-19 agenda item 1.13. The parameters have been chosen to match the given BS cell sizes.

[6] These values are established based on reasonable assumptions.

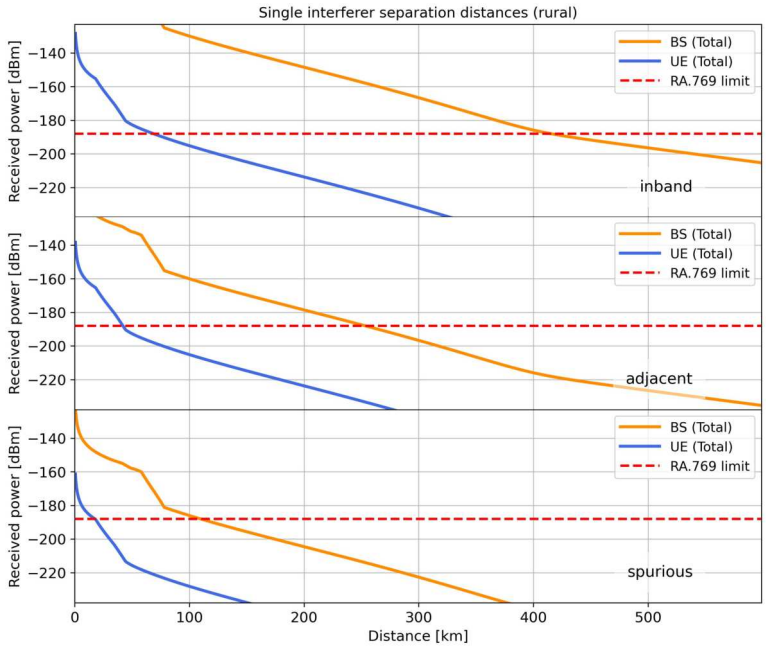

Figure 13: Received power at RAS station in the spectral line RAS band (50kHz) for rural case, generic scenario: red (BS); blue (UE)

In Table 8, the results for the generic site are comparable to those for the Medicine site. This is due to the flat terrain surrounding the observatory, where the signal encounters few obstacles. Although SRT and Noto are well shielded by the surrounding mountains, the expected coordination zone is quite large for in-band cases and progressively narrowing for the adjacent and spurious case.

Table 8: Coordination zone result provided by single case interference of Italian radiotelescope for BS. The calculated distances are based on maximum distances from RT site.

	Generic site	**Medicina**	**SRT**	**Noto**
in-band	410 km	>300 km	300 km	>300 km
adjacent	250 km	290 km	200 km	120 km
spurious	106 km	150 km	20 km (up to 200 km in one direction)	20 km (up to 150 km in one direction)

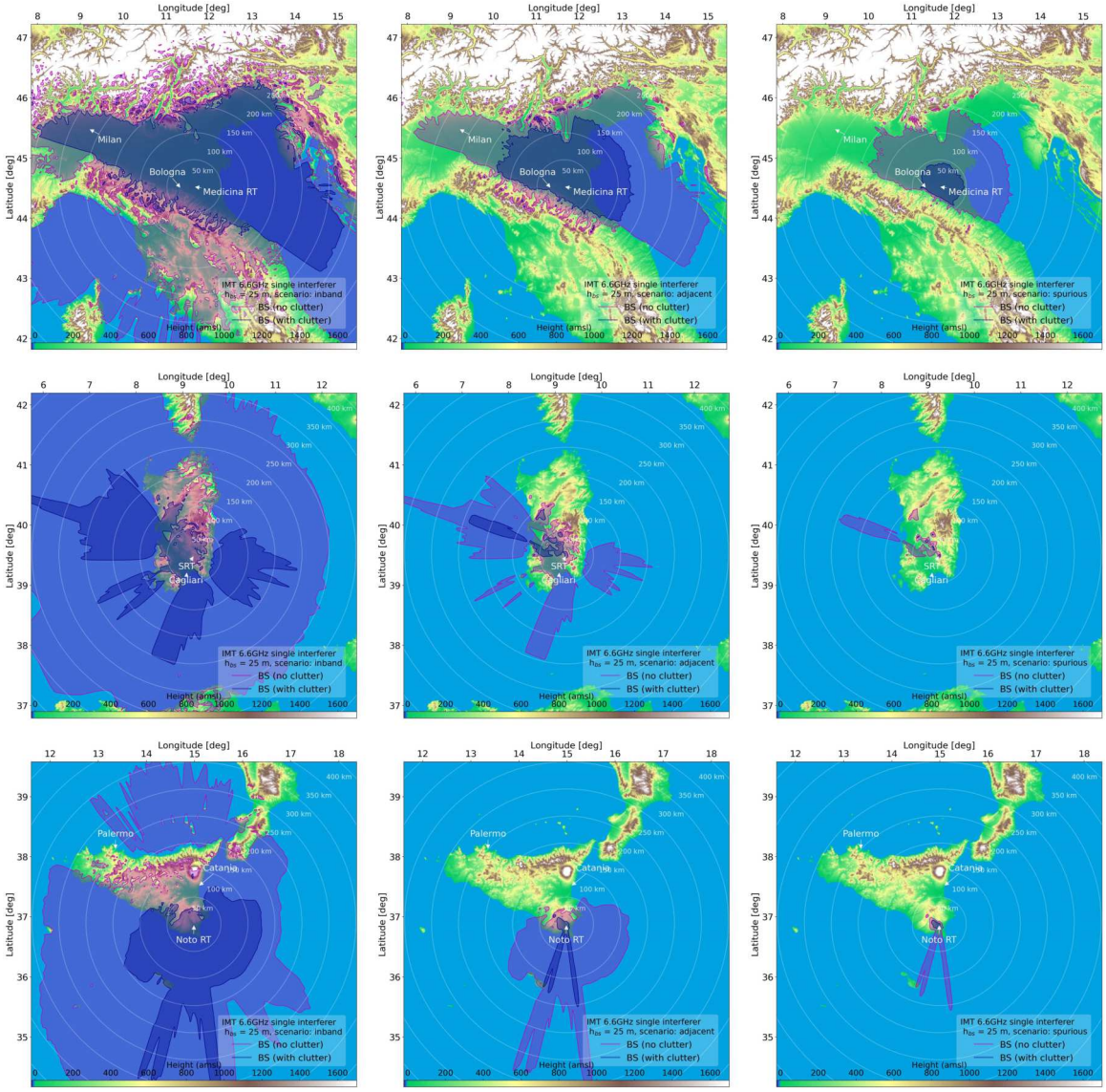

Figure 14: IMT BS coordination zone with RAS (6650-6675.2 MHz) for in-band (first column), adjacent (second column), and spurious (third column) scenarios. Clutter loss is considered in the blue curve, but not in the red curve.

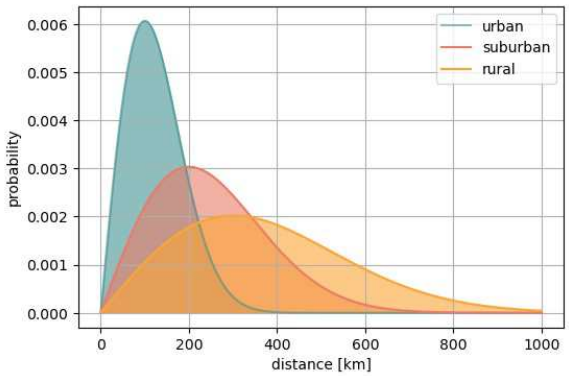

Figure 15: UE distribution around the base station (BS) for each scenario (urban, suburban, rural

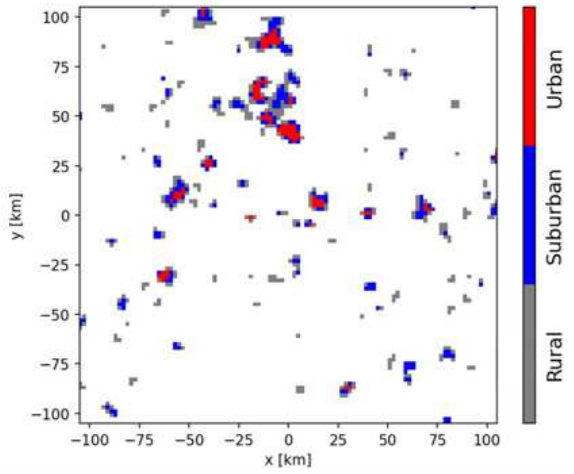

Figure 16: Clustered distribution of BSs

4.4 Aggregated scenario

Aggregated data requires treatment that is much more complex. First, random devices are deployed around the radio telescope. An area large enough to estimate the total power received by the radiotelescope is considered. A number of variables were taken into account, such as the antenna down-tilt for enhanced beam directivity, and beamforming efficiency, which reduces by 20% from in-band to spurious scenarios.

The positioning of UE and BS is critical for overall system performance and is often modelled using a probability distribution. The Rayleigh distribution is commonly used to model the distance between UEs and BSs, which determines their positioning as a function of radial distance, as shown in Figure 15.

The placement of BSs in suburban and urban scenarios typically does not follow the Rayleigh distribution but clusters in the most populated areas. A cluster deployment is considered as shown in Figure 16

Figure 17 shows a typical network layout. On the left, points represent UE, and their colour rep-

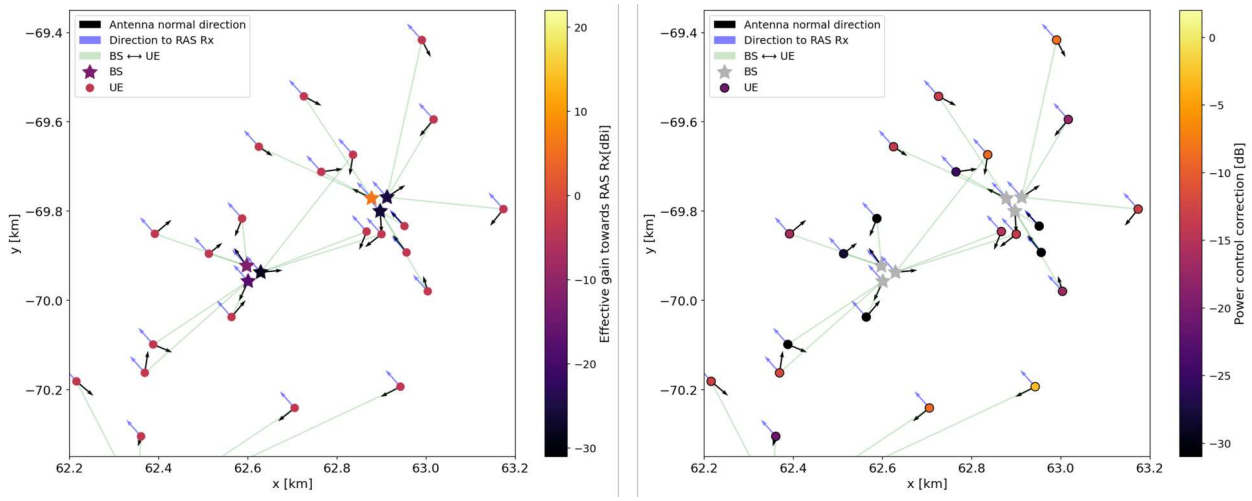

Figure 17: Left: Effective Gain towards RAS of UE and BS. Right: Power control correction for each UE

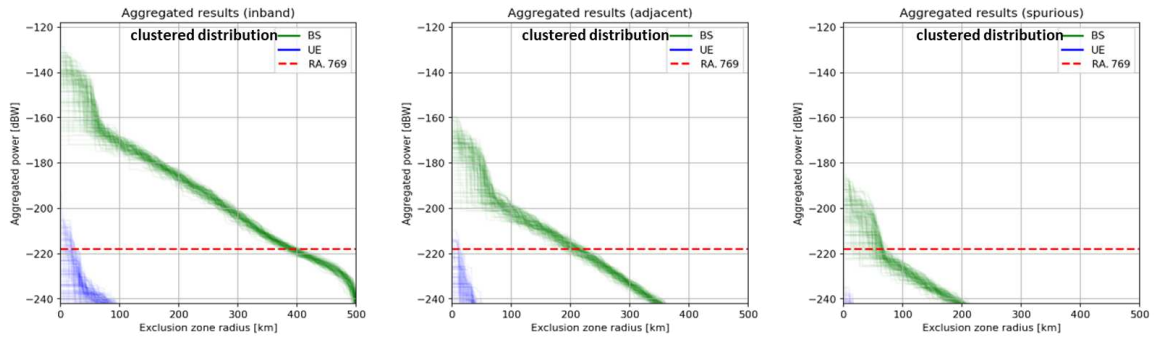

Figure 18: Coordination zone radius results for IMT for aggregated simulation for generic case

resents the effective gain towards RAS which appears on the top left of the map (RAS is not displayed). On the right, the effect of power control on UE output levels is shown: UE devices are coloured by output power after the power control algorithm. As proof of this, points near the BS require less power than those far away (dark). The green lines indicate the connection between UE and BS.

The Monte Carlo simulation is used to perform aggregate simulation, where each iteration represents a different configuration of UE and BS inside the designated area. The received power level at the RAS station is calculated by summing up the emitted power levels of each individual device and accounting for the antenna gains and propagation losses. However, in most cases, this results in interference levels that exceed the RAS threshold levels. As with car radar analysis, the exclusion zone is computed using the same approach. The simulations are performed for various distribution scenarios, including uniform and cluster density, as well as different domains, such as adjacent, spurious, and in-band. The results of the aggregated scenario are presented in Figure 18. Due to the differing approach between the single and aggregate cases, making a direct compari-

Table 9: Summary of the exclusion zone radii of BS and UE for generic aggregated and generic single-case scenario

	inband		adjacent		spurious	
	Single case scenario	**Aggregated scenario**	**Single case scenario**	**Aggregated scenario**	**Single case scenario**	**Aggregated scenario**
BS (km)	415	407	253	230	109	70
UE (km)	68	25	17	12	17	1
BS+UE (km)	n/a	407	n/a	230	n/a	70

son between the results of them is not straightforward. For a single case, the coordination zone is depicted on a map. In contrast, for aggregate cases, the coordination zone is presented as a function depending on the distance from the radiotelescope. However, an order of magnitude of the coordination zone for BS is shown in Table 9.

The findings indicate that even in spurious cases, separation distances greater than 50 km are required to avoid harmful interference, while in in-band cases, separation distances of up to 400 km may be necessary. However, the UEs do not contribute to the aggregate total received power.
RAS analysis has not considered the terrain profile of a specific site, and shows alarming results, especially for methanol observations. The primary source of interference comes from BS, which are usually installed at higher altitudes and transmit significantly more power. The calculated coordination zones for in-band scenarios are extensive, reaching up to 400 km for BS and about 70 km for UE. The difference between the coordination zones in the UE device between the single scenario and the aggregated one for the inband case can be traced back to clutter. In fact, for the single case, clutter was not taken into consideration since it is the worst case scenario. These results indicate that European scientists will be unable to observe methanol from the stars. Additionally, the spurious case demonstrates that ensuring compatibility between IMT and RAS in the 6.6 GHz band is challenging, with a distance of around 60 km to maintain compatibility with the threshold power level for harmful interference recommended by ITU-R RA.769. Another issue needs to be addressed is the use of this frequency band by neighbouring countries. If some countries do not intend to use this band for IMT, their radio telescopes may still experience interference from neighbouring countries, a situation known as cross-border interference.

5 Compatibility Study between RLAN and RAS

5.1 Scientific interests and regulatory status of the 6.6 GHz band

WAS/RLAN (Wireless Access System/ Radio Local Area Network) is a wireless communication technology that connects devices to a local area network (LAN) using radio waves.
WAS/RLAN systems can provide wireless coverage in a wide range of locations, including commercial and residential buildings, as well as hospitals. These systems are commonly employed to deliver high-speed internet connectivity in enterprise, commercial, and industrial settings. In particular, RLAN creates wireless networks in buildings and campuses for multiple devices, while WAS provides internet access in a limited area (for simplicity in this report, WAS will be also referred to as RLAN device). The RLAN devices item includes numerous devices of various nature such as telephones, televisions, IoT devices, but also external wireless connections to cover public areas with Wi-Fi. Currently, there are around 19 billion active Wi-Fi devices, and that number is expected to grow in the near future. Like IMT, RLAN is also interested to use the frequency spectrum in the upper 6 GHz band by extending the frequency range from the current 5.925 – 6.425 GHz to 5.925 – 7.125 GHz. In addition to having typically lower transmission heights and powers than IMT devices (BS and UE), RLAN devices typically use the unlicensed bandwidth. Licence types should not be underestimated. The administration typically provides a limited number of licences for specific locations, and in the case of the BS, which is the most problematic device to guarantee compatibility for IMT, its exact location should be known beforehand.

5.2 Compatibility study

In this report, the focus is on the aggregate scenario where numerous devices are deployed near the RAS station. Since the most device is located indoor, an analysis based on a single case scenario with weak transmitter power would not be realistic. The detailed study was presented to the CEPT SE45 [25]. Similarly to the previous cases presented in this report, a detailed analysis is conducted for three radio astronomical sites in Italy: SRT, Medicina and Noto. Actual population densities and land cover types are taken into account for realistic results. Such datasets are available with high quality and sufficient spatial resolution at all European RAS sites.
In aggregation simulations, a number of RLAN devices are randomly sampled in a box around a specific RAS site, based on the aforementioned population density and with a range of transmitter heights above ground (reflecting the likelihood of devices on several floors of buildings). A small fraction of the devices is intended for outdoor use (with less shielding), but it is assumed that the majority will be used indoors. In the next step, the individual path propagation losses between the transmitters and the RAS receiver are calculated. All powers received in each instance of time are added and averaged over the typical observation/integration time at the radio telescope (2000 seconds) and finally compared with the allowed threshold levels. To study the typical statistical uncertainty of the simulation, the simulation is repeated several times, which makes possible to study the posterior distribution (pool results).

5.2.1 RAS and transmitter parameters

In line with previous studies, protection criteria for RAS are defined in Recommendation ITU-R RA.769-2. As discussed in the IMT section, RAS is primarily performing studies in the 6.65 GHz band (6650-6675.2 MHz). Transmitted power levels of RLAN devices vary significantly due to wide range of applications and therefore, for an aggregation scenario, a distribution of output powers is assumed according to Table 10. A combination of Low Power Indoor (LPI) RLANs with power

Table 10: LPI/VLP outdoor power distributions. (Source: ECC Report 316, Table 2)

Tx eirp power	200 mW	100 mW	50 mW	25 mW	13 mW	12.5 mW	3.25 mW	1.0 mW	Total
Indoor	9.81%	6.24%	26.01%	0%	52.31%	0%	0%	5.63%	100%
Outdoor[1]	0%	0%	0%	6.93%	0%	45.71%	47.36%	0%	100%

Note 1: For outdoor deployment, an additional body loss of 4 dB is to be applied.

Table 11: Bandwidth distribution. (Source: ECC Report 302, Table 12)

Channel bandwidth	20 MHz	40 MHz	80 MHz	160 MHz
WAS/RLAN device percentage	10%	10%	50%	30%

levels up to 200 mW and outdoor Very Low Power (VLP) portable RLANs with power levels up to 25 mW is used in the report. The same is true for the actual channel bandwidths, which are listed in Table 11. It's crucial to highlight that while certain RLAN devices can achieve a maximum transmitter power of 1000 mW, the data source, as referenced in [26], enforces a limit of 200 mW. Nevertheless, it's important to point out that even when simulating a small percentage of devices operating at 1000 mW (lower than 0.3%), this has a minimal effect on the overall results.

For outdoor deployment, an additional body loss of 4 dB is applied.

5.2.2 Population density for spatial device deployment

The spatial distribution of devices in the simulation can be controlled using population density maps. These maps indicate the density of people in a given grid cell, which is proportional to the number of RLAN devices found in that cell. For example, people connect to these networks at work or at home, as well as in shopping malls and restaurants.
The NASA Socioeconomic Data and Applications Center (SEDAC) offers a worldwide population density map called the "Gridded Population of the World" (GPW) data set, which is available in Version 4 under Creative Commons Attribution 4.0 International (CC BY 4.0) licence. Figure 19 visualizes the UN WPP-Adjusted Population Density (v4.11; year 2020) for the Medicina RAS station. Although the GPW-4 grid has high angular resolution (grid cells have about 30 arcseconds, or 1 km, at the equator), only average values are used for each county or city in the region shown on the map. This should not be a concern for the wide simulated area. To generate a population map better suited for random sampling of devices, the density map is multiplied by the area of each grid cell. This results in a scaled version of the density map. However, the curvature of the Earth causes some inhomogeneity in grid cell area. To address this issue, the "inverse sampling technique" is used to generate random samples of longitude and latitude pairs that conform to the population distribution function. The total number of desired active devices in the target area must be provided to use this method.

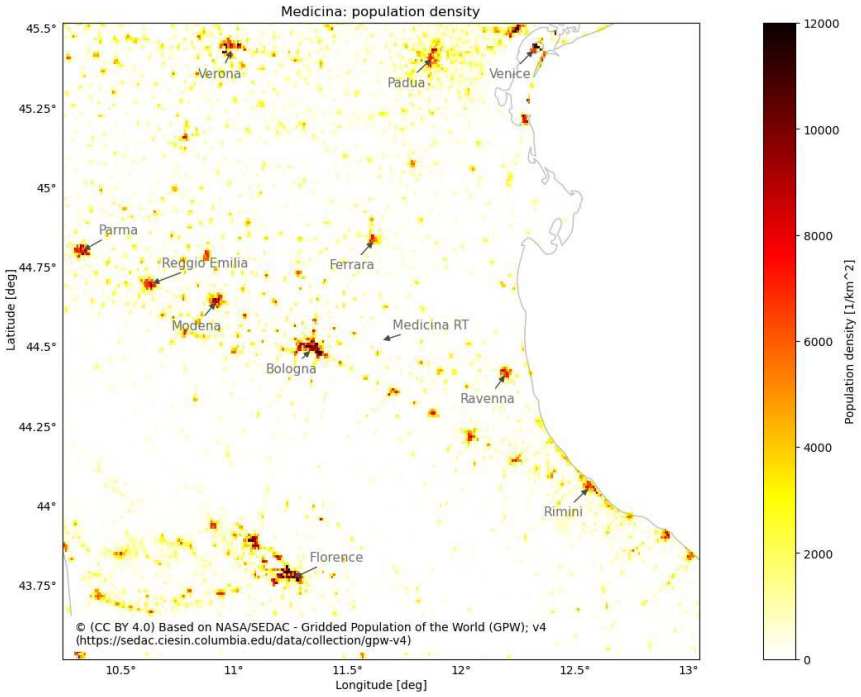

Figure 19: Population density around Medicina observatory

Table 12: Number of transmitter devices for both low and high usage scenarios

RAS Station	Simulation box size	Total population	Active devices	
			Low	High
SRT	2°×2°	1.19 Mio	270	676
Medicina	2°×2°	10.47 Mio	2376	5960
Noto	2°×2°	2.88 Mio	653	1639

5.2.3 Aggregated Case

In the simulation, the population (density) map is used for spatial deployment, i.e., sampling the locations of devices. This requires knowing the number of active transmitters in the simulated box which is 1 deg^2 (about 110 km × 110 km) in this case. Furthermore, the activity factor is derived from ECC Reports 302 and 316; see Table 12. It depends on factors such as the estimated market adoption factor, the percentage of devices in the 6-GHz band (in comparison to all bands), and busy hours. Multiplying all percentages yields the activity factor. This number is multiplied by the population count to determine the total number of active devices. The number of devices in the simulated area is listed in Table 12 according to the different use scenarios ("Low", and "High").
An antenna installation height is then assigned to each sampled device location (based on ECC report 302, table 10). It is further assumed that 99% of the devices are indoors and only 1% are outdoors (for further details see ECC Report 316 [26], Section 4.2.1.2). This is a little different from the 98% and 2% figures that were reported in ECC Report 302.
A visual representation of the sampling transmitter for high usage scenario can be found in Figure

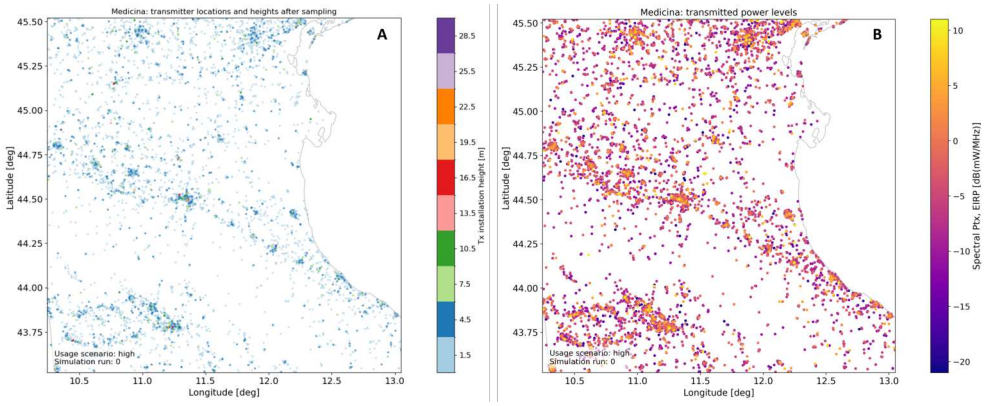

Figure 20: A: The distribution of transmitters based on height at Medicina site; B: Power levels transmitted by each device (EIRP)

20 A.
As expected, the spatial distribution follows the population density map. Each device is randomly assigned a power level according to Table 10 and Table 11, see Figure 20 B.
To determine the received powers at the RAS station, the path propagation loss, building entry loss (BEL), and clutter loss must be determined for each device. The path propagation losses and clutter losses depend on the antenna installation heights and the clutter zone type. However, most radio telescopes are either situated much higher than surrounding clutter or in open terrain. As said before, clutter loss according ITU-R P.2108 was calculated considering the transmitter site of the propagation path.
The building entry losses, according to Rec. ITU-R P.2109, depend on the propagation path's elevation angle, which is calculated using the Rec. ITU-R P.2109 procedures. This involves specifying the frequency, outdoor radiation elevation angle, and building type, as well as the desired probability. The Rec. ITU-R P.2109 covers frequencies between 80 MHz and 100 GHz and considers two types of building construction: traditional and thermally efficient. The majority of devices experience clutter losses between approximately 15 and 20 dB, with less than 10% of devices experiencing no significant clutter attenuation. Building entry losses peak at approximately 20 dB, but have a relatively flat distribution; see Figure 21. BEL for outdoor devices is 0 dB by definition.
The received power of each device is calculated by subtracting path propagation, clutter, and building entry losses from the transmitted power. One iteration of the simulation may result in aggregated power being below the threshold established by Rec. ITU-R RA.769. However, in some circumstances, the received power may exceed this threshold. By chance, there may be one or more transmitting devices located close to the RAS station (particularly if the RLAN device is located outdoors). This analysis is performed by repeating the simulation 2000 times, which allows us to analyse typical statistical scattering in the results. A distribution of one iteration of the received power is shown in Figure 22. Compared to all devices, outdoor devices are few, according to ECC Report 316 [26]. The maps of received power at RAS station are shown in Figure 23.
Since some simulation runs yield aggregated powers that exceed the RAS limits, a minimum separation distance for coexistence is needed in the 6650.0–6675.2 MHz band. A coordination zone with a growing radius is applied, i.e., all devices within the coordination zone radius are excluded when computing aggregated power. For each simulation, the blue curves show aggregated power. Solid black lines indicate the median considering both indoor and outdoor devices. As a compari-

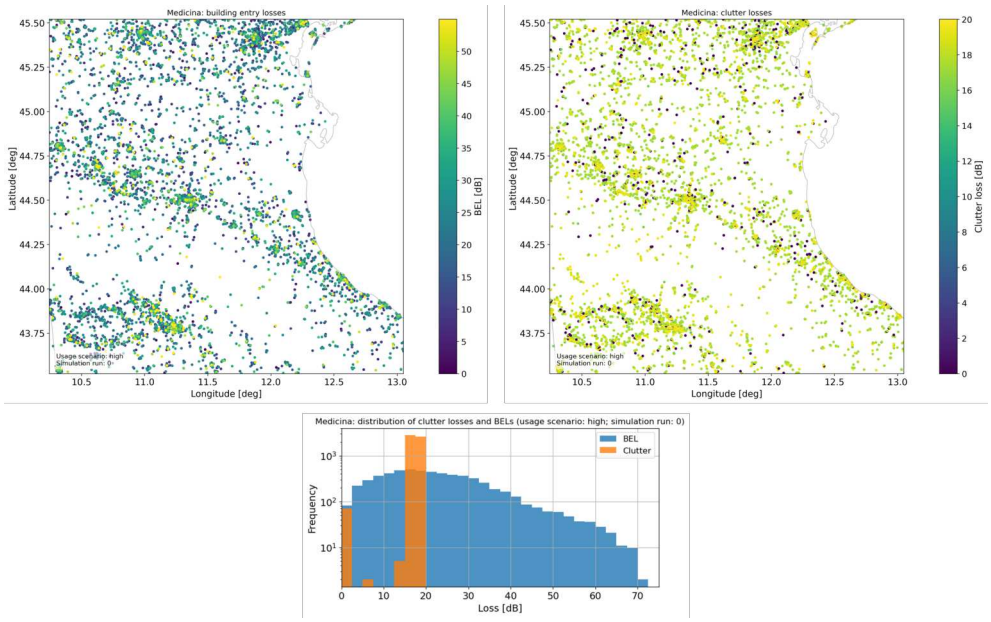

Figure 21: Other loss considered in the simulations. Top: BEL and clutter loss for each device. Bottom: Building entry loss and clutter histogram

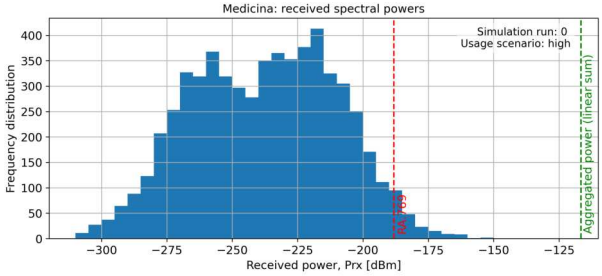

Figure 22: The distribution of received powers at the RAS station. Green vertical line indicates aggregated spectral power; red vertical line indicates RAS threshold levels defined in Rec ITU-R RA.769

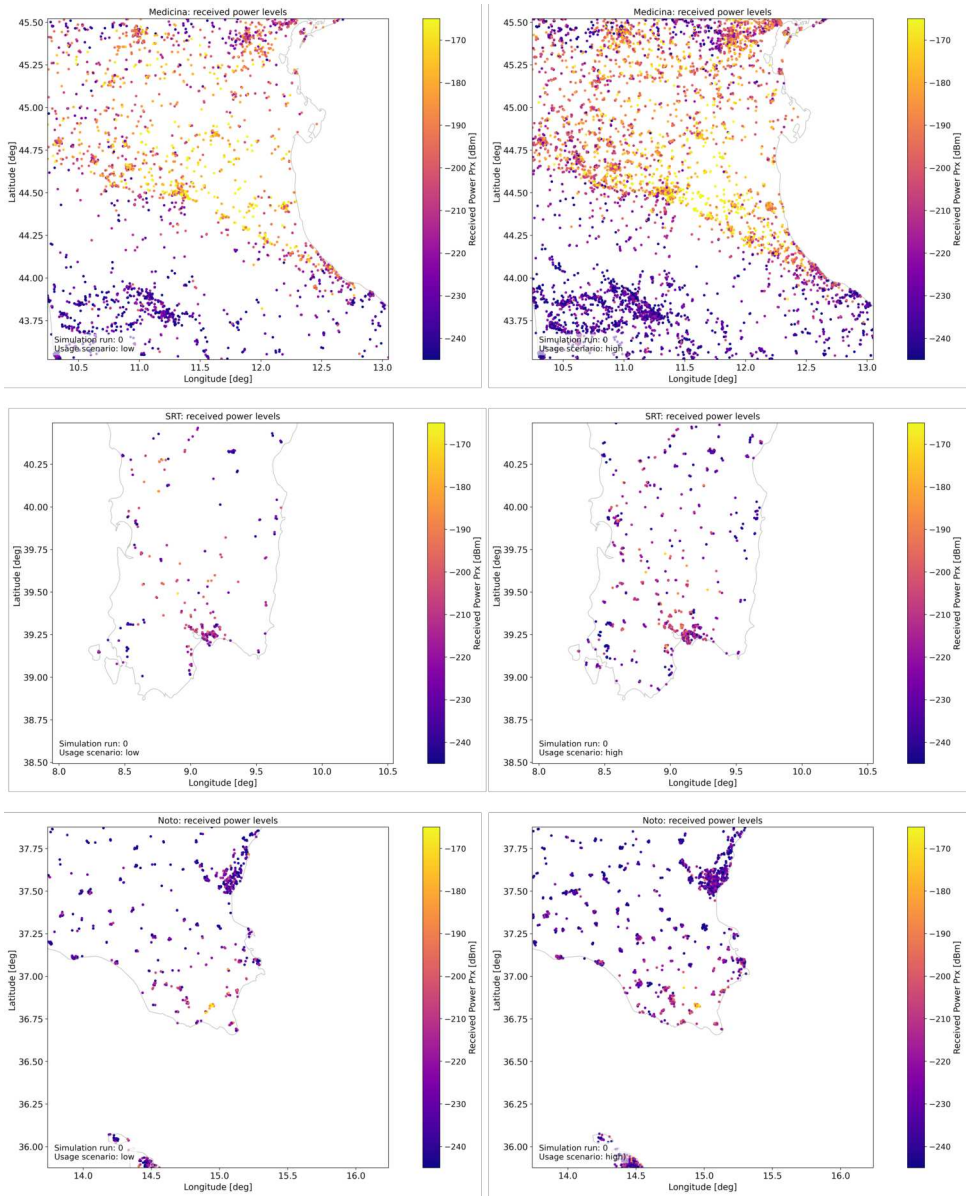

Figure 23: Received power level at RAS station for low (left) and high (right) usage scenario

Table 13: Summary of coordination zone for RLAN applications

	Scenario (outdoor + indoor devices)	
Site	**Low usage**	**High usage**
SRT	2 km	23 km
Noto	8 km	9 km
Medicina	>70 km	>70 km

son, Figure 24 displays the results of the simulations for both "low" and "high" usage scenario. As a comparison, there are also curves coloured in grey for indoor-only devices. The total aggregated power is dominated by outdoor installations.

According to the results of the RLAN analysis, the coordination zone necessary to avoid interference with RAS strongly depends on the location of the radio telescope and therefore on the density of the population there. Furthermore, the presence of outdoor devices strongly increases the size of the coordination zone. In comparison to IMT, RLAN has a smaller coordination zone in the 6.6 GHz band. Due to its flat terrain, only the Medicina site has a large coordination zone. The site of SRT and Noto allow a coordination zone of about ten/twenty kilometres.

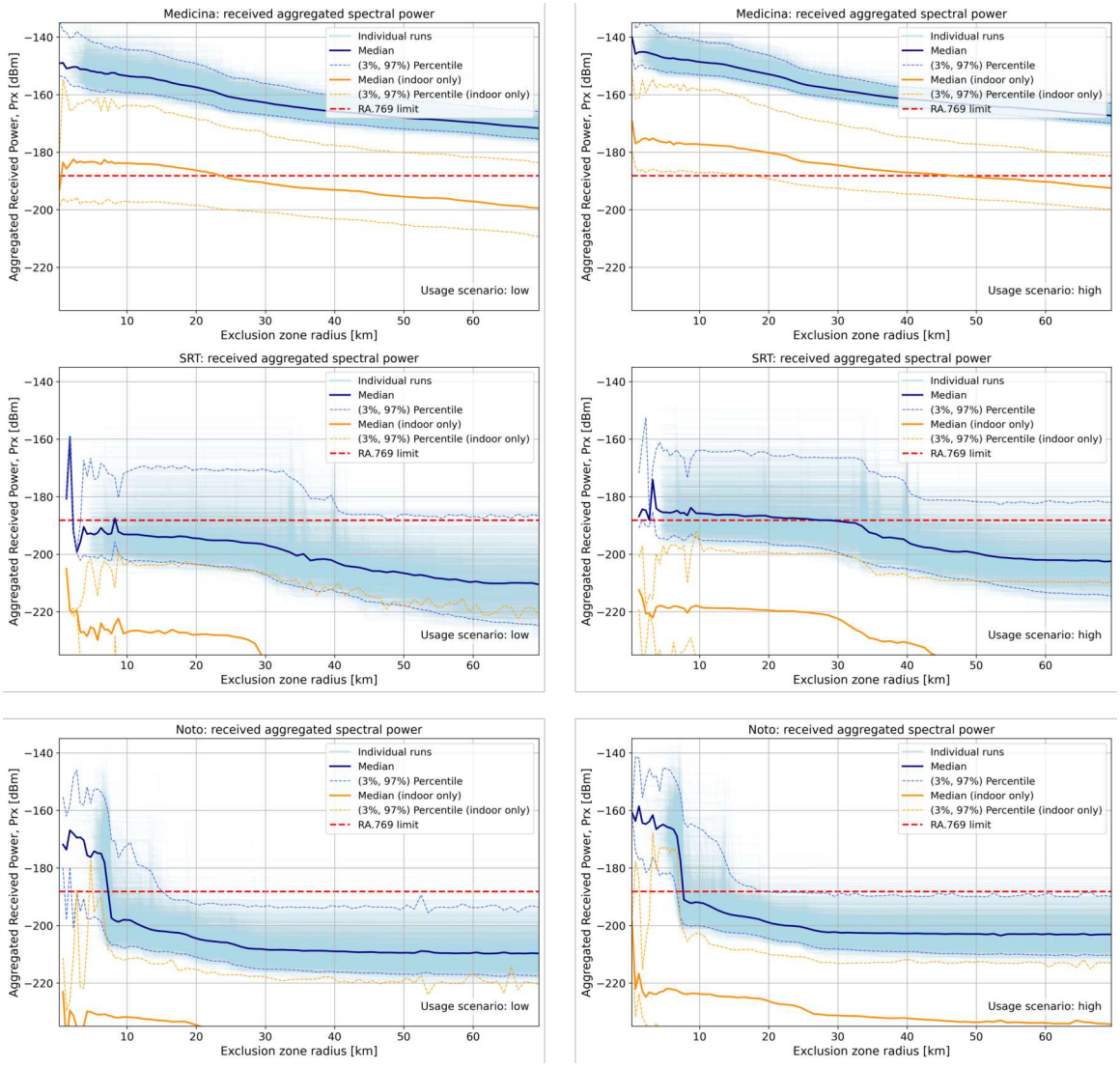

Figure 24: Aggregated received power for SRT (top), Medicina (middle) and Noto (bottom) for low (left) and high (right) usage scenario.

6 Conclusions

The purpose of this report is to illustrate potential services that could interfere with radio astronomy observations and provide tools for how to remediate them.
Table 14 summarize the assumptions and types of simulations. Part of the table contains several blank boxes because some scenarios were not designed to be easy to read. This table is not intended to be fully completed, as plenty of hypothesizes could be done. While Table reftable-summary2 in this report illustrates extrapolations of the coordination zones for the technologies under discussion.
The significance of conducting precise compatibility studies for car radar, IMT, and RLAN applications has been affirmed through recent analyses. Such studies become even more crucial in light of RAS vulnerability and allow for aggregate assessments to yield more realistic outcomes. All simulations shown are conducted using a pycraf software tool, which allows for the rapid integration of features relevant to RF analysis, including antenna models, elevation maps, and clutter identification, with highly reliable results. It has been established that the SRT and Noto sites are more resistant to interference, attributed to their terrain profiles, compared to the Medicina site. Regarding the compatibility with car radars at 77 GHz, tens of km of the coordination zone is required even considering only the front radar. As regards compatibility with 6.6 GHz, the coordination zone for IMT devices is greater than for RLAN devices, primarily due to the use of internal transmitters and lower. It's important to clarify that IMT allocation would typically involve licensed usage, whereas RLAN allocation would be typically unlicensed. In the latter scenario, there would be no important information, such as the number and position of the devices operating near the radio telescopes. The lack of such information makes coordination very difficult.Therefore, the RAS community does not advocate for a particular service, but instead emphasizes the need for protection with respect to any potential service that may arise.

Table 14: Summary of types of studies and assumptions used in the analysis

Study	**Note**	**Car Radar (77 GHz)**	**IMT (6.6 GHz)**	**RLAN (6.6 GHz)**
Generic Site, Single case	No clutter, no extra loss	-	yes	-
Site Specific, Single case	No clutter, no extra loss	yes	yes	-
Generic Site, Aggregate case	No clutter, no extra loss	-	yes	-
Site Specific, Aggregate case	yes clutter loss, yes extra loss (BEL)	yes	-	yes

Simulation case	Simulation type	Generic site	Medicina	SRT	Noto
Car Radar (Radar type A)	Single	-	30 km	30 km	10 km
	Aggregated	-	65 km	34 km	15 km
IMT (BS-inband)	Single	410 km	415 km	>300 km	300 km
	Aggregated	415 km	-	-	-
RLAN (high-usage scenario)	Single	-	-	-	-
	Aggregated	-	>70 km	28 km	8 km

References

[1] B. Winkel, *pycraf - compatibility studies for radio astronomy spectrum management*,. URL: https://pypi.org/project/pycraf/

[2] ITU Radio Regulations, Edition of 2020 https://www.itu.int/pub/R-REG-RR

[3] Recommendation ITU-R P.452-16 (07/2015) *Prediction procedure for the evaluation of interference between stations on the surface of the Earth at frequencies above about 0.1 GHz*

[4] Recommendation ITU-R P.676-11 (08/2022) *Attenuation by atmospheric gases and related effects*

[5] Recommendation ITU-R P.835-6 (12/2017) *Reference standard atmospheres*

[6] ©Corine Land Cover (CLC), URL: https://www.copernicus.eu.

[7] "Noto, I: Regione Siciliana: MDT 2012-2013 2×2 ETRS89; Licence: Creative Commons Attribution 4.0 International (CC BY 4.0)," URL: `https://www.sitr.regione.sicilia.it/geoportale/mobile/search.html`.

[8] "SRT, I: Regione Autonoma della Sardegna, Sardegna Geoportale: DTM 1 m and DTM 10 m Licence: Creative Commons Attribution 4.0 International (CC BY 4.0)," [Online]. URL: `https://www.sardegnageoportale.it/webgis2/sardegnamappe/?map=download_raster`.

[9] "Shuttle Radar Topography Mission (SRTM)," URL: `https://www2.jpl.nasa.gov/srtm/`.

[10] "Medicina, I: Regione Emilia-Romagna: DTM 5×5 2014; Creative Commons Attribution 3.0 International (CC BY 3.0),". URL: `https://geoportale.regione.emilia-romagna.it/catalogo/dati-cartografici/altimetria/layer-2`.

[11] Recommendation ITU-R RA.769-2, (05-2003) *Protection criteria used for radio astronomical measurements*

[12] Recommendation ITU-R RA.1513-2, (03-2015) *Levels of data loss to radio astronomy observations and percentage-of-time criteria resulting from degradation by interference for frequency bands allocated to the radio astronomy service on a primary basis*

[13] ECC Decision, *ECC Decision of 12 November 2004 on the frequency bands to be designated for the temporary introduction of Automotive Short Range Radars (SRR)* "ECC/DEC/(04)10" 2004.

[14] Report ITU-R M.2322-0, (11-2014) *Systems characteristics and compatibility of automotive radars operating in the frequency band 77.5-78 GHz for sharing studies*

[15] Report ITU-R RA.2457-0, (06-2019) *Coexistence between the radio astronomy service and radiolocation service applications in the frequency band 76-81 GHz*

[16] ECC Report 350 (02-2023), "Radiodetermination equipment for ground based vehicular applications in 77-81 GHz,"

[17] OpenStreetMap contributors, *Planet dump retrieved from `https://planet.osm.org`* URL: `https://www.openstreetmap.org`

[18] "opendatacommons,". URL: `https://opendatacommons.org/`

[19] CEDR (Conference of European Directors of Roads), "Trans-European Road Network, TEN-T (Roads): 2019 Performance Report," 2019.

[20] Recommendation ITU-R M.2057-1, (2018-01), "Systems characteristics of automotive radars operating in the frequency band 76-81 GHz for intelligent transport systems applications".

[21] CRAF, CEPT ECC PT1, *AI 1.2-related studies IMT vs RAS* (2021) URL: ECC PT1(21)229

[22] Annex 4.4 to Working Party 5D Chairman's Report, "Characteristics of terrestrial component of IMT for sharing and compatibility studies in preparation for WRC-23," Jun. 2021

[23] Task Group 5/1 Chairman's Report (Annex 1, Document 5-1/478 (Annex 1), Study Period (2015-2019)

[24] Table 5.4.4.2-3 3GPP TR 37.840 (01-2014) *Study of Radio Frequency (RF) and Electromagnetic Compatibility (EMC) requirements for Active Antenna Array System (AAS) base station (Release 12)*

[25] CRAF, SKAO, CEPT ECC SE45, *RAS sharing and compatibility*. (2022) URL: SE45(22)015

[26] ECC Report 316 (03-2020) *Sharing studies assessing short-term interference from Wireless Access Systems including Radio Local Area Networks (WAS/RLAN) into Fixed Service in the frequency band 5925-6425 MHz*

[27] Table 8.1.2-1 and equation 8.1.2-4 ETSI TR 138 921 V17.1.0 (2022-05) Study on International Mobile Telecommunications (IMT) parameters for 6.425 – 7.025 GHz, 7.025 – 7.125 GHz and 10.0 – 10.5 GHz (3GPP TR 38.921 version 17.1.0 Release 17)